

People's Democratic Republic of Algeria  
Ministry of Higher Education and Scientific research  
M'hamed Bougara University, Boumerdes  
Institute of Electrical and Electronic Engineering,  
**Laboratory of Signals and Systems (LSS)**



# ALGERIAN JOURNAL OF SIGNALS AND SYSTEMS

**ISSN : 2543-3792**

**Title: Broken Rotor Bars Fault Detection Based on Envelope Analysis Spectrum and Neural Network in Induction Motors**

**Authors: Saddam BENSOUCHA<sup>(1)\*</sup>, Sid Ahmed BESSEDIK<sup>(2)</sup>, Aissa AMEUR<sup>(2)</sup>, Abdellatif SEGHIOR<sup>(1)</sup>**

**Affiliation:**

**<sup>(1)</sup> Laboratoire d'Etude et Développement des Matériaux Semi-Conducteurs et D'électriques (LeDMaSD), Université Amar Telidji de Laghouat, Algérie, BP 37G, Route de Ghardaïa. 03000, Laghouat, Algérie**

**<sup>(2)</sup> Laboratoire d'Analyse et de Commande des Systèmes d'Energie et Réseaux Electriques (LACoSERE), Université Amar Telidji de Laghouat, Algérie, BP 37G, Route de Ghardaïa. 03000, Laghouat, Algérie**

**Page range: 106-116**

## **IMPORTANT NOTICE**

**This article is a publication of the Algerian journal of Signals and Systems and is protected by the copyright agreement signed by the authors prior to its publication. This copy is sent to the author for non-commercial research and education use, including for instruction at the author's institution, sharing with colleagues and providing to institution administration. Other uses, namely reproduction and distribution, selling copies, or posting to personal, institutional or third party websites are not allowed.**

**Volume : 3 Issue : 3 (September 2018)**

Laboratory of Signals and Systems

Address : IGEE (Ex-INELEC), Boumerdes University, Avenue de l'indépendance, 35000, Boumerdes, Algeria

Phone/Fax : 024 79 57 66

Email : lss@univ-boumerdes.dz ; ajsyssig@gmail.com

# Broken Rotor Bars Fault Detection Based on Envelope Analysis Spectrum and Neural Network in Induction Motors

Saddam BENSOUCHA<sup>(1)\*</sup>, Sid Ahmed BESSEDIK<sup>(2)</sup>, Aïssa AMEUR<sup>(2)</sup>, Abdellatif SEGHIOUR<sup>(1)</sup>

<sup>(1)</sup> Laboratoire d'Etude et Développement des Matériaux Semi-Conducteurs et D'électriques (LeDMaSD), Université Amar Telidji de Laghouat, Algérie, BP 37G, Route de Ghardaïa. 03000, Laghouat, Algérie

<sup>(2)</sup> Laboratoire d'Analyse et de Commande des Systèmes d'Energie et Réseaux Electriques (LACoSERE), Université Amar Telidji de Laghouat, Algérie, BP 37G, Route de Ghardaïa. 03000, Laghouat, Algérie

Emails: s.bensaoucha@lagh-univ.dz<sup>(1)\*</sup>, s.bessedik@lagh-univ.dz<sup>(2)</sup>, a.ameur@lagh-univ.dz<sup>(2)</sup>, a.seghiour@lagh-univ.dz<sup>(1)</sup>

**Abstract:** In this paper, a study has presented the performance of a neural networks technique to detect the broken rotor bars (BRBs) fault in induction motors (IMs). In this context, the fast Fourier transform (FFT) applied on Hilbert modulus obtained via the stator current signal has been used as a diagnostic signal to replace the FFT classic, the characteristics frequency are selected from the Hilbert modulus spectrum, in addition, the different load conditions are used as three inputs data for the neural networks. The efficiency of the proposed method is verified by simulation in MATLAB environment.

**Keywords:** Induction motors, Broken rotor bars, Faults detection, Envelope analysis, Neural networks

## 1. INTRODUCTION

Squirrel-cage induction motors (SCIMs) are the most popular motors used in the industrial processes where this machine consumes about 85% of the total energy. These machines have many advantages, among which mention their robust structure, easy design, cheap costs and low maintenance requirements [1]-[3].

Despite these advantages, owing to the thermal electrical and mechanical stresses, also the environmental stresses, electrical and mechanical faults are unavoidable in SCIMs [4]-[7]. These faults vary according to their type and location, and classified as follows [1]-[8]:

- The stator windings faults or single phasing fault (30–40% of full faults);
- The BRBs faults, segment and ring faults in SCIMs (5–10%);
- The mechanical faults where bearing faults are the most frequent fault (40–50%).

In this context, several changes to motor current signals may occur due to these faults, generates unbalanced in stator currents and its voltages, unbalanced in rotor currents and its voltages, unbalanced in the torque pulsation, reduces the electromagnetic torque, augmentation the speed fluctuations of the motor, increasing in the temperature and the vibration in this machine [1]-[8].

In BRBs case, the detection of this fault is one of the most difficult, because the SCIM keeps working without any perceivable change may indicate a fault at the level of this machine [8].

As results of this fault, the stator current harmonics components around the fundamental frequency ( $f_s$ ) and its multiples are increasing, in addition, due to bars breakage adversely affect progressively the health of the neighboring bars [1]-[9].

In some sensitive industrial areas, reliability demands for electric motors are constantly increasing due to some of the important motor applications. Therefore, correct diagnosis and early detection of incipient faults result in fast unscheduled maintenance and short downtime for the process under consideration [10]. For these reasons, many studies dealt with the problem of BRBs detection and diagnosis through different techniques.

In general, the motor current signatures analysis (MCSA) technique is considered the most promising faults detection method [6], [8], [11] - [14], this technique has many advantages, the most important advantages are [15], [17], and [23]:

- It does not require the estimation of machine parameters;
- This technique is capable to provide the machine states without requiring access to the machine (inexpensively).
- This method allows diagnosing the state of the IMs without having to stop this machine (online detection).

MCSA technique is noninvasive, and the current sensor is commonly used in the industrial process as by electrical engineers [3]. Often, MCSA technique using motor currents and vibration signals, then the obtained signals will be analyzed using various methods such as the fast Fourier transform (FFT), Zoom FFT, and short-time Fourier transform, discrete Fourier transform [16]-[19], in addition, Park vector approach (PVA) [18]-[20] and discrete wavelet transform [3],[4], the multiple signal classification [18], [21], estimation of signal parameters via rotational invariance techniques [26], envelope detection obtained by PVA or Hilbert transform (HT)[15], [17]-[19], [23]. As a result, MCSA has become the standard for online detection of the faults, one of the most widely used techniques to obtain information on the health state of the machine is based on the processing of the stator currents lines [6], [13], [20]. Many studies based on FFT have been conducted over the years to detect the BRBs. In FFT-based, the spectrum of stator currents can be used to diagnose the faults in IMs [5]. A large amount of research has been directed toward using the stator current spectrum (classical FFT) to detect the motor faults [7], [13],[20][22].

Unfortunately, this technique shows a severe lack of diagnostic accuracy, especially in BRBs fault diagnosis, the major drawbacks of FFT classic are [16], [18]:

- FFT classic is influenced by many factors, including electric supply, the load conditions, motor geometry, these factors may lead to indicate a false alarm detection;
- Often, IMs use speed control devices, which adversely affect the effectiveness of the diagnosis by using FFT classic (increasing the signal noise);
- FFT classical-based usually requires a long acquisition time to achieve a high spectral resolution and a high sampling frequency to reduce aliasing effects;
- However, this technique generates a huge amount of data, which makes its implementation difficult using embedded devices with small internal memory, such as digital signal processors or devices with low computing power.

To resolve these problems, the envelope analysis based on HT or PVA was used to obtain the stator current envelope (SCE), FFT-based applied on this SCE to extract the features related (harmonics frequency) to indicate a motor fault [7], [15],[20],[22], the problems of spectral leakage and memory space has been solved by using this SCE [15], [22].

In [7], [16], [22] the authors used the spectrum of the Hilbert modulus (HM) in order to diagnose of stator faults. In [22], [23], the authors use the FFT of HM for BRBs diagnosis. In [11], a procedure was presented used two types of stator currents, FFT used the stator current line and FFT applied on HM for BRBs fault detection, the Hilbert spectrum was used to diagnose bearings fault in [24]. The SCE spectrum by FFT used Park modulus (PM) has been discussed in [23], the author relied on this signal to diagnose the stator fault, and also the author adopted the same method (PM) to diagnose the BRBs fault.

Based on these works, the section one of this paper is presented two studies comparative in order to BRBs detection, FFT using HM, then, FFT applied on PM signal.

In FFT classic, the monitoring of BRBs based on MCSA to detect sidebands harmonics frequency  $f_b$  around the fundamental supply frequency  $f_s$  expressed by  $f_b = (1 \pm 2ks)f_s$ , with  $s$  : is the slip and  $k = 1, 2, 3, \dots$  is positive integer [1], [12], [15].

As mentioned earlier, the traditional FFT method suffers from several imperfections, however, the components  $f_b$  are relatively close to the fundamental frequency ( $f_b \approx f_s$ ) when the IMs is operating at low slip.

A solution for this problem, the SCE spectrum analysis by FFT using HM or PM is a good tool for IMs dynamic fault analysis since it increases resolution, this technique can accurately detect BRBs when the SCIM is operating at very low load, and needs very little storage [15], [22], [24]. The SCE spectrum is used to compute the instantaneous amplitudes  $Af_{bb}$  and instantaneous frequency  $f_{bb}$

[15], [21]-[24] given by  $f_{bb} = 2ksf_s$ .

Unfortunately, the results obtained by SCE (HM or PM) spectra are given by the complex spectrum modulus, the interpretation the harmonics results content analysis is very difficult and could not be done easily by MCSA methods (MSCA) [6],[15],[26]. To overcome this limitation, artificial intelligence techniques (AITS) have numerous advantages to diagnose the different faults of the IMs [23], [5], these techniques are easy to extend and modify, these can be made adaptive by the incorporation of new data or information, besides giving improved performance [23].

In recently years, AITS have been introduced using concepts such as expert systems (ES) [26], the adaptive neural fuzzy inference systems (ANFISs) [27], support vector machines (SVMs) [20],[28],[29], fuzzy logic systems (FLS) [4],[10],[12],[30], artificial neural networks (ANNs) [22],[26],[30], genetic algorithms (GAs) [6].

Extracting the best features from the signal processing may be the most important basic procedure of AITS to arrive at an effective diagnosis of the state of the SCIM because it directly affects the performance of these techniques to identify the nature of the faults [26] - [31].

In section two of this paper, the technique proposed and based on AITS. In particular, ANN technique applied for BRBs fault detection in SCIM, it's based on using the results of the HM spectrum, and the load conditions  $T_L$  to identify the different states in this SCIM (section III).

## 2. BROKEN ROTOR BARS MODELING IN SQUIRAL CAGE INDUCTION MOTOR

The model presented in this section is specific to a SCIM, this machine has a set of the three-phase stator winding, the rotor is composed of  $N_r$  identical rotor bars and two segment end rings. The model of a SCIM in the reference frame  $(d, q)$  axis related to the rotor is defined as below [29], [30]:

- Voltage equations in stator parties:

$$\begin{bmatrix} V_{ds} \\ V_{qs} \end{bmatrix} = \begin{bmatrix} R_s & -w_r L_{sc} & 0 & -N_r w_r M_{sr} & 0 \\ w_r L_{sc} & R_s & -N_r w_r M_{sr} & 0 & 0 \end{bmatrix} \begin{bmatrix} i_{ds} \\ i_{qs} \\ i_{dr} \\ i_{qr} \\ i_e \end{bmatrix} + \begin{bmatrix} L_{sc} & 0 & \frac{-N_r M_{sr}}{2} & 0 & 0 \\ 0 & L_{sc} & 0 & \frac{N_r M_{sr}}{2} & 0 \end{bmatrix} \frac{d}{dt} \begin{bmatrix} i_{ds} \\ i_{qs} \\ i_{dr} \\ i_{qr} \\ i_e \end{bmatrix} \quad (1)$$

- Voltage equations in rotor parties:

$$\begin{bmatrix} V_{dr} \\ V_{qr} \\ V_e \end{bmatrix} = \begin{bmatrix} 0 \\ 0 \\ 0 \end{bmatrix} = \begin{bmatrix} 0 & 0 & R_r^{11} & R_r^{12} & 0 \\ 0 & 0 & R_r^{21} & R_r^{22} & 0 \\ 0 & 0 & 0 & 0 & R_e \end{bmatrix} \begin{bmatrix} i_{ds} \\ i_{qs} \\ i_{dr} \\ i_{qr} \\ i_e \end{bmatrix} + \begin{bmatrix} -\frac{3}{2} M_{sr} & 0 & L_{rc} & 0 & 0 \\ 0 & \frac{3}{2} M_{sr} & 0 & L_{rc} & 0 \\ 0 & 0 & 0 & 0 & L_e \end{bmatrix} \frac{d}{dt} \begin{bmatrix} i_{ds} \\ i_{qs} \\ i_{dr} \\ i_{qr} \\ i_e \end{bmatrix} \quad (2)$$

Where:  $V_{dqs}, V_{dqr}, V_e$  and  $i_{dqs}, i_{dqr}, i_e$  are the stator, the rotor and the end ring segment voltages and its courants in axis  $(d, q)$  respectively.

$L_{sc}, L_{rc}$  and  $L_e$  are the cyclic inductances of stator, rotor, and end ring segment respectively.

$R_s$ : are the stator windings resistances,  $M_{sr}$  are the stators to rotor mutual inductances.

$R_r^{11}, R_r^{12}, R_r^{21}, R_r^{22}$ : are the rotor windings resistances and  $N_r$  is number of rotor bars.

$R_e$ : is the end ring segment inductance,  $w_r$  is the angle speed between rotor and stator.

The state of the rotor bars depends on Eq. 2, for a healthy SCIM:

$$\begin{cases} R_r^{11} = R_r^{22} = R_r = 2 \frac{R_e}{N_r} + 2Rb(1 - \cos \alpha) \\ R_r^{21} = R_r^{12} = 0 \end{cases} \quad (3)$$

In presence the BRBs:

$$R_r^{11} = R_r^{22} = \frac{2}{N_r} \left[ \left( \frac{2R_e}{N_r} + Rb_1 + Rb_{N_r} \right) \cos^2 1\beta + \left( \frac{2R_e}{N_r} + Rb_2 + Rb_1 \right) \cos^2 2\beta + \dots + \left( \frac{2R_e}{N_r} + Rb_{N_r} + Rb_1 \right) \cos^2 N_r \beta \right] - \frac{4}{N_r} \left[ (Rb_1 \cos 1\beta \cos 2\beta) + (Rb_2 \cos 2\beta \cos 3\beta) + \dots (Rb_{N_r} \cos N_r \beta \cos 1\beta) \right] \quad (4)$$

$$R_r^{12} = R_r^{21} = -\frac{2}{N_r} \left[ \left( \frac{2R_e}{N_r} + Rb_1 + Rb_{N_r} \right) \cos^2 1\beta + \left( \frac{2R_e}{N_r} + Rb_2 + Rb_1 \right) \cos^2 2\beta + \dots + \left( \frac{2R_e}{N_r} + Rb_{N_r} + Rb_1 \right) \cos^2 N_r \beta \right] + \frac{2}{N_r} \left[ (Rb_1 \cos 1\beta \sin 2\beta) + (Rb_2 \cos 2\beta \sin 3\beta) + \dots (Rb_{N_r} \cos N_r \beta \sin 1\beta) \right] + \frac{2}{N_r} \left[ (Rb_1 \sin 1\beta \cos 2\beta) + (Rb_2 \sin 2\beta \cos 3\beta) + \dots Rb_{N_r} \sin N_r \beta \cos N_r \beta \right] \quad (5)$$

For example, for obtaining a break in the first and second bars, must be increased the value of the resistance bar number one ( $Rb_1$ ) and two ( $Rb_2$ ) through a positive coefficient  $\eta$  given according to the following formula  $Rb_1^* = \eta.Rb_1$  and  $Rb_2^* = \eta.Rb_2$ ; where:  $\eta$  positive integer ( $\eta \geq 11$ ),  $Rb_1^*$  and  $Rb_2^*$  are new bar resistances that the first and second bar takes after the fault in this bars.

With:  $\beta = (2\pi / N_r)$  is the electrical angle of two adjacent rotors meshes.

The equation describing the mechanical part of the system is:

$$T_e - T_L = J \frac{d\Omega_r}{dt} - f_d \Omega_r \quad (6)$$

Where:  $T_e$  is the electromagnetic torque produced by the motor,  $T_L$  is the load torque applied on the motor,  $J$  is the rotor inertia,  $\Omega_r$  is the rotor angular speed,  $f_d$  is coefficient of damping.

The expression of the electromagnetic torque is given by:

$$T_e = p(i_{qs}\phi_{dr} - i_{ds}\phi_{qr}) \quad (7)$$

Where:  $\phi_{dqr}$  is the rotor flux according to axis ( $d, q$ ) and  $p$  presented a number of pole pairs.

### 3. SIMULATION RESULTS WITH BROKEN ROTOR BARS FAULTS

In order to study the influence of the BRBs number on the SCIM, SCIM simulations are performed on 3-phase, 4-pole, 1.1kW and 220/380V, the motors operate under rated load at  $\Omega_n = 1425 \text{ rpm}$ .  $\eta = 20$ ,  $Rb_1 = Rb_2 = 6.1 \times 10^{-6} \Omega$ . The system parameters of the motor tasted in this study are given by Table. I.



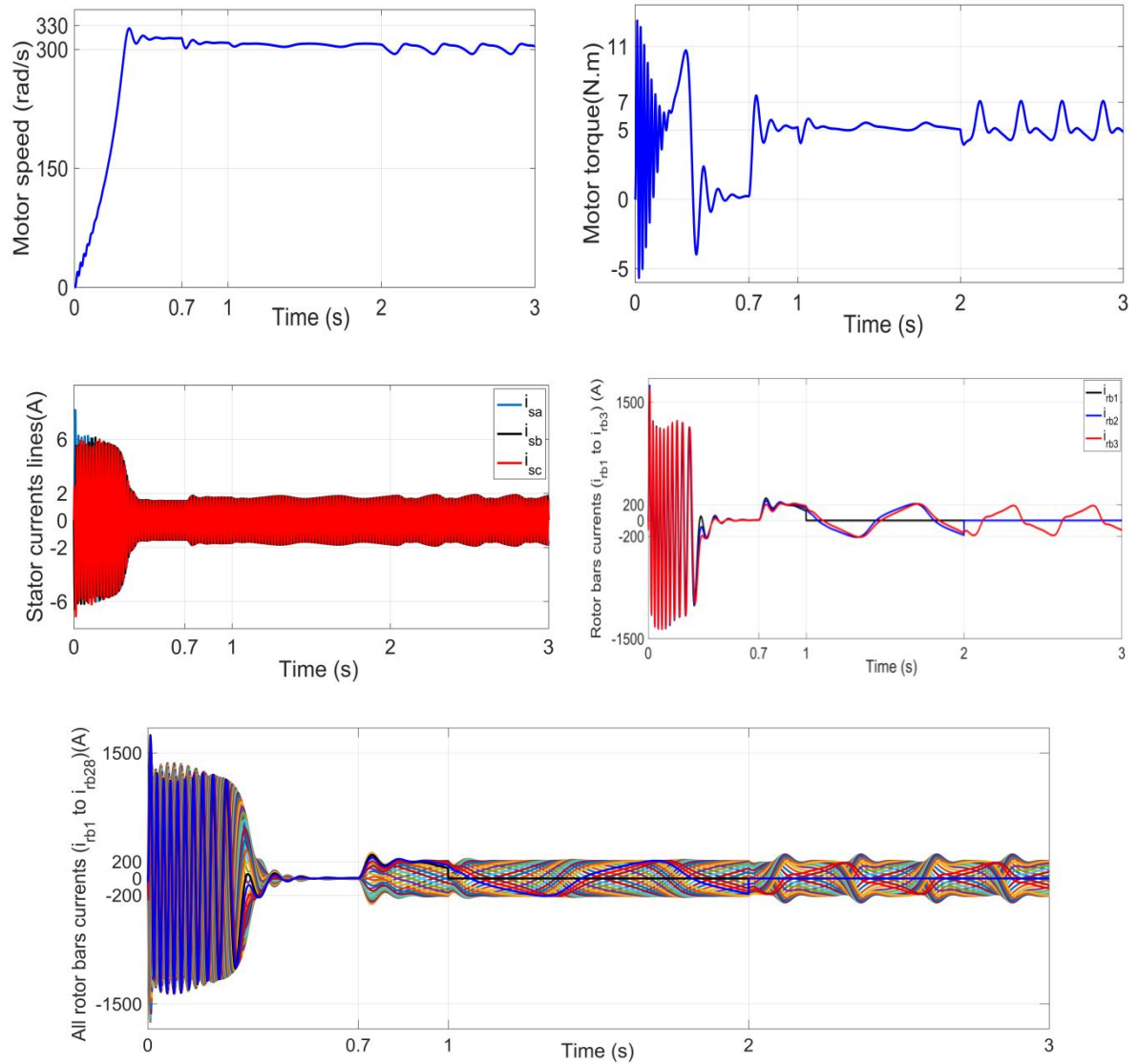


Fig.1 Simulation results of the squirrel cage -induction motor .heallhty rotor (0 to 1s), one broken rotor bar (1 to 2s) and two broken rotor bars(2 to 3s) under a torque load ( $T_L=5\text{N.m}$  at 0.7s).

As illustrated in Fig.1, the BRBs show oscillations on speed and the motor torque, as well as stator currents, the increase of BRBs causes an increase in the amplitude of oscillations of these curves, in other hand, the currents in the broken bars fall to zero while currents in the neighboring bars unbalanced.

#### 4. APLICATION THE PARK,HILBERT TRANSFORM TO DETCTION THE BRBS FAULT

##### A. Park transform analysis

As a function of the three- phase currents  $i_{s\_abc}(t)$  , the currents of Park  $i_{dq}(t)$  can be calculated by means of the following two relations as below [18], [19], and [23]:

$$\begin{cases} i_d(t) = \sqrt{\frac{2}{3}}i_{s\_a}(t) - \sqrt{\frac{1}{6}}i_{s\_b}(t) - \sqrt{\frac{1}{6}}i_{s\_c}(t) \\ i_q(t) = \sqrt{\frac{2}{3}}i_{s\_b}(t) - \sqrt{\frac{1}{2}}i_{s\_c}(t) \end{cases} \quad (8)$$

Based on Eq.8, the envelope analysis shown in the Fig.2 for modulated signals using Park transform is defined as:

$$i_{Park} = \sqrt{i_d^2(t) + i_q^2(t)} \quad (9)$$

### B. Hilbert transform Analysis

Mathematically, HT is defined as a convolution with the function  $(1/t)$ , as follows [15], [17], [23], [30]:

$$HT(x(t)) = y(t) = \frac{1}{\pi t} \times x(t) = \frac{1}{\pi} \int_{-\infty}^{+\infty} \frac{x(\tau)}{t - \tau} d\tau \quad (10)$$

Based on stator current phase  $i_{s-a}(t)$ , Eq.10 is defined as below:

$$i_{hilbert} = y(t) = \frac{1}{\pi t} \times i_{s-a}(t) = \frac{1}{\pi} \int_{-\infty}^{+\infty} \frac{i_{s-a}(\tau)}{t - \tau} d\tau \quad (11)$$

The divergence at  $(t = \tau)$  is allowed for by taking the Cauchy principal value of the integral.

Eq.11 enables to create an artificial complex signal  $Z(t)$  is defined by:

$$Z(t) = i_{s-a}(t) + y(t) \quad (12)$$

Where:  $y(t)$  is the result of HT applied on signal phase  $i_{s-a}(t)$ .

The instantaneous amplitude  $A_z(t)$  and the instantaneous phase  $\varphi_z(t)$  are given by Eq.13:

$$\begin{cases} A_z = \sqrt{i_{s-a}^2(t) + y^2(t)} \\ \varphi_z(t) = \arctan(y(t) / i_{s-a}(t)) \end{cases} \quad (13)$$

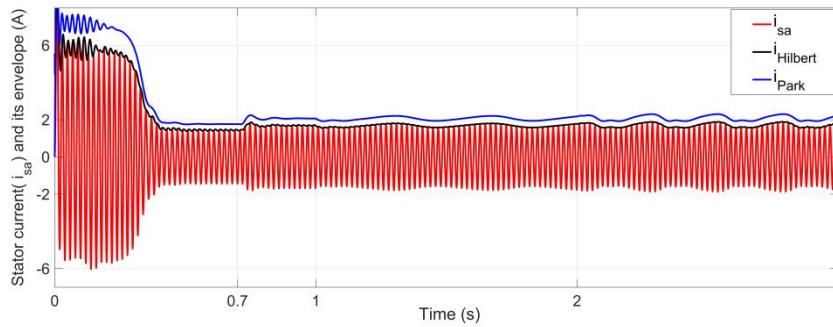


Fig.2 Stator current phase  $i_{s-a}(t)$ , Hilbert modulus and Park modulus with healthy rotor (0 to 1s), one broken rotor bar (1 to 2s) and two broken rotor bars (2 to 3s) under a torque load ( $T_L=5N.m$  at 0.7s).

As presented in Fig.2, the PM and HM shows a pulsation with the characteristic of the state of the motor either healthy machine and with BRBs faults.

### C. FAST FOURIER TRANSFORM APPLIED ON PARK, HILBERT MODULUS

In this section, a study is presented to compare the performance of BRBs detection using FFT of PM, FFT of HM in order to determine and extract the BRBs related features ( $f_{bb}$ ,  $Af_{bb}$ ), the acquisition time  $T_s = 9s$  (1 to 10s), with a sampling frequency  $F_e = 10kHz$  for all the experiments in Hanning window.

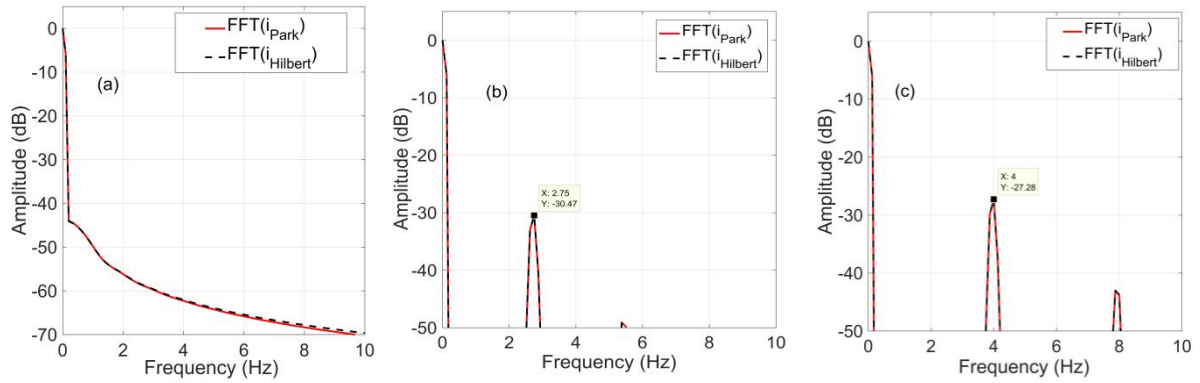


Fig. 3 FFT spectrum applied on Hilbert modulus and Park modulus .(a) healthy rotor,(b) one broken rotor bar and (c) two broken rotor bars under a torque load  $T_L=5N.m$  .

The envelope analysis using HM or PM contains a continuous component ( $2k.f_s$ ) generated by the fundamental component of the stator current as a result of breaking in bars , the most two frequency compensates are  $2sf_s$  and  $4sf_s$  respectively [18], these components are shown clearly in Fig. 3(b) and Fig. 3(c). Through the results illustrated in Fig. 3, it is clear that the FFT spectrum applied to the envelope analysis (HM, PM) make the same result in the different states of the motor. Although PM can be presented the same results to obtain by using HM, the high cost due to the requirement to use three current sensors associated with an advanced processing technique (see Eq.8), unlike HM, they need one signal phase so they need to one sensor of the stator current (Eq.11).As a result of this, in this paper, we will rely the results obtained by FFT-based using HM for its use with ANN technique for detection the BRBs as shows in Fig.4.

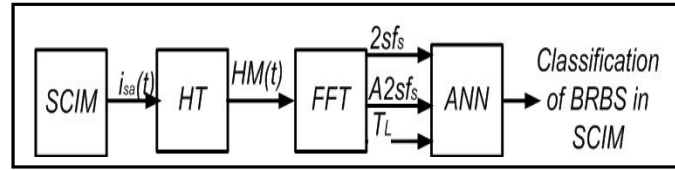


Fig.4 Structure of BRBs fault diagnosis based on Hilbert modulus spectrum and artificial neural network.

## 5. ROTOR FAULT DETECTION USING NEURAL NETWORK VIA HILBERT MODULUS

Basically, the ANN represents a nonlinear system referring to its input-output behavior, this nonlinear transformation results from the inner structure of a neural network, the ANN is presented as a "black box" that receives input signals and provides the appropriate responses[29]. In general, several parametric studies were conducted for ANNs. There were a total of three main steps:

- Choice input-output variables;
- Construction of the ANN;
- Classified the database obtained to train, test, and validation ANN selected.

ANN-based require a training process in order to make efficient fault detection thanks to all data collected (inputs) from the simulation results of the motor in order to monitor its state.

In this paper, the main goal of to use ANN approach in BRBs fault detection and to better distinguish between these symptoms (a healthy motor, one BRB, two BRBs), the adopted ANN is a feed forward multi-layers perceptron (MLPs), this MLPs consist of an inputs layer represented of source nodes, hidden layers of computation nodes and an output layers, the number of nodes in the inputs and the outputs layers depend on the number of inputs and outputs variables respectively, these structures affect directly on the generalization capability of the ANN. ANN is using back propagation algorithm (BPA), where BPA is one of the most powerful learning algorithms in NN [27]. The feed forward MLP neural network, used in this work, consisted of three layers: three inputs, one hidden layer with three neurons using Tangent sigmoid transfer function, one output layer (Fig.5). In this context, based on ANN technique, the extracted features ( $2sf_s$ )



and its amplitude ( $A2sf_s$ ) from HM spectrum (based on FFT spectra) also the load conditions applied on the SCIM are used as inputs of ANN in order to classified the state of this SCIM.

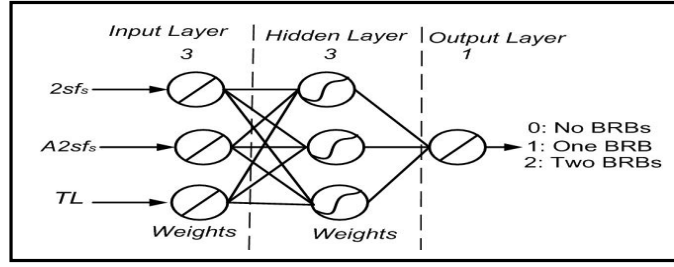


Fig. 5 Artificial neural network structure to broken rotor bars fault detection.

#### A. Simulation results: train, test and the validation of neural network detection

The select inputs data set is collected through simulations by Matlab, under different operating conditions of the SCIM.

The training step is composed by a successive range of 12 samples representing three states of the operating conditions of the IM under four load conditions ( $T_L = 1;3;5;7N.m$ ) is defined as:

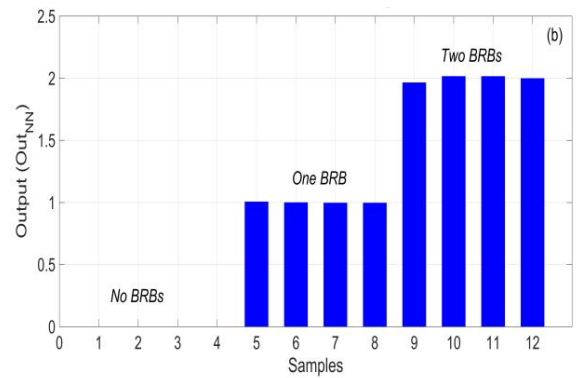
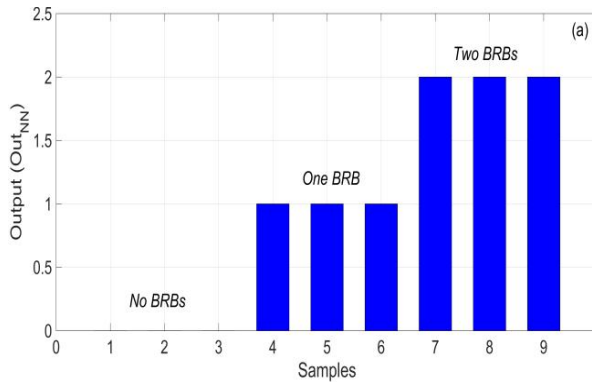
- Four samples ( $2sf_s; A2sf_s$ ) with healthy motor (No BRBs);
- Four samples ( $2sf_s; A2sf_s$ ) with one BRB;
- Four samples ( $2sf_s; A2sf_s$ ) with two BRBs.

The test step is composed by a successive range of 9 samples representing three states of the operating conditions of the IM under three load conditions ( $T_L = 2;4;6N.m$ ) is defined as:

- Three samples ( $2sf_s; A2sf_s$ ) with healthy motor ;
- Three samples ( $2sf_s; A2sf_s$ ) with one BRB ;
- Three samples ( $2sf_s; A2sf_s$ ) with two BRBs.

The validation step is composed by a successive range of 12 samples representing three states of the operating conditions of the IM under four load conditions ( $T_L = 1.5;2.5;3.5;4.5N.m$ ) :

- Four samples ( $2sf_s; A2sf_s$ ) with healthy motor ;
- Four samples ( $2sf_s; A2sf_s$ ) with one BRB;
- Four samples ( $2sf_s; A2sf_s$ ) with two BRBs.



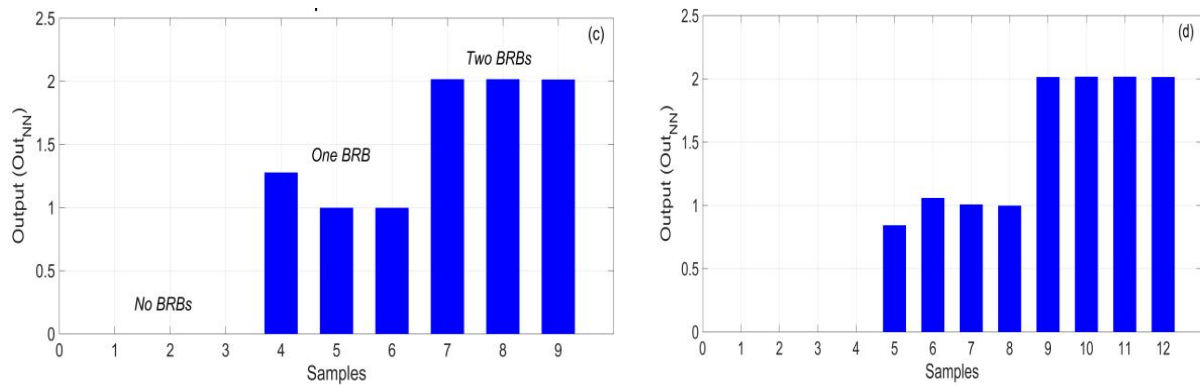


Fig. 6 Artificial neural network simulated results .(a) the Target of NN training,(b)the output of NN training,(c)the output of NN test and (d) the output of NN validation .

Through the desired and training outputs of ANN are shown in Figs. 6(a) and “Fig. 6(b), respectively, shows that the training errors are very low, proving that the NN has well learned the inputs data and has correctly reproduced the desired output.

As shown in Figs.6(c), based on the test result of the system, it is clear that this ANN allowed the detection of the states of the motor in its different conditions, the same is true for the generalization step where the system proved effective to find the type of fault (No BRBs, One BRBs or two BRBs)Fig.6(d).

The mean square error (MSE) is defined as comparing the difference between the outputs produced by the ANN compared to the desired results (targets). However, the normalized of this MSE is calculated and propagated backwards to adjust the value of the weights on the neural connection in the MLP [28].

In this work, this process was repeated 5000 epochs until the MSE was reduced to an acceptably low value (0.00014671) suitable to classify the test set correctly as shown below.

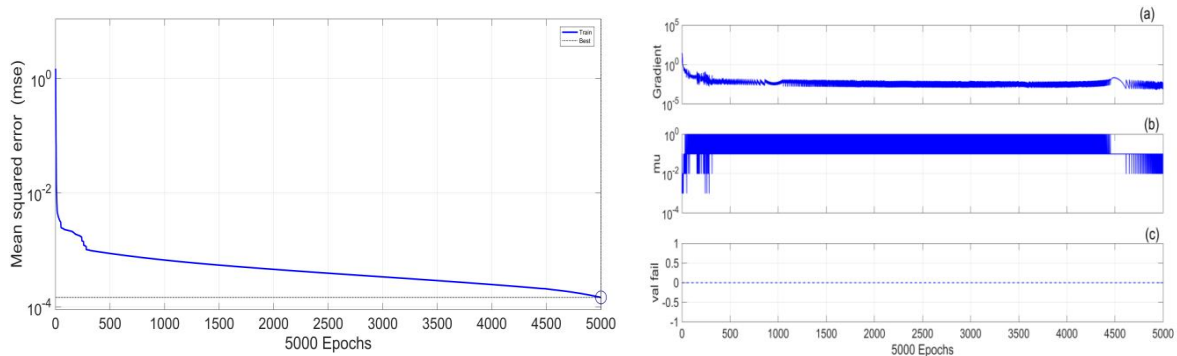


Fig.7 ANN training performance MSE (left), the NN training state (right), (a) Gradient = 0.00067849, (b) Mu=0.1, and (c) Validation Checks = 0 at epochs 5000.

## 6. CONCLUSION

This paper presents a method combines between the Hilbert transform and the neural network to detect automatically the broken rotor bars fault of the squirrel cage induction machine.

The envelope analysis spectrum using Hilbert modulus is a good tool for detecting the BRBs when the SCIM is operating at low slip. This signal analysis can be used to detect other faults such as the stator faults, mechanical faults in this machine. Using Hilbert modulus spectrum, a diagnosis technique was adopted a neural networks in order to detect the numbers of BRBs in SCIM, this technique has been shown to be very effective for detecting and classifying the different states of

the motor (healthy state, BRBs fault) under various conditions. The simulation results demonstrate the effectiveness of the proposed technique to detect the number of BRBs.

Table 1 Squirrel cage induction motor parameters

	Variable parameters	Values
$P_n$	Output power	1.1KW
$V_s$	Supply voltage	220/380V
$f_s$	Supply frequency	50Hz
$I_n$	Rated current	2.6/4.3A
$\Omega_n$	Nominal speed	1425rpm
$p$	Number of pole pairs	2
$R_s$	Stator resistance	9.81 $\Omega$
$R_r$	Rotor resistance	3.83 $\Omega$
$R_e$	Resistance of end ring segment	$5.6 \times 10^{-7} \Omega$
$R_b$	Rotor bar resistance	$6.1 \times 10^{-7} \Omega$
$L_e$	Inductance of end ring	$17 \times 10^{-7} \Omega$
$M_{sr}$	Mutual inductance	$1.73 \times 10^{-4} H$
$N_s$	Number of turns per stator phase	464
$N_r$	Number of rotor bars	28
$J$	Inertia moment	0.0125k.g.m <sup>2</sup>
$f_d$	Coefficient of damping	0.00119 N.m / rad.s

## References

- [1] S. Karmakar, S. Chattopadhyay, M. Mitra, S. Sengupta, "Induction Motor Fault Diagnosis," Publisher Springer Singapore, 2016.
- [2] S. A. Saleh and E. Ozkop, "Phaselet-Based Method for Detecting Electric Faults in  $\phi$  Induction Motor Drives—Part I: Analysis and Development," in IEEE Transactions on Industry Applications, vol. 53, no. 3, pp. 2976-2987, May-June 2017.
- [3] P. Shi, Z. Chen, Y. Vagapov, Z. Zouaoui, "A new diagnosis of broken rotor bar fault extent in three phase squirrel cage induction motor," Mechanical Systems and Signal Processing, vol. 42, no 1-2, p. 388-403. 2014.
- [4] M. M. Rahman and M. N. Uddin, "Online Unbalanced Rotor Fault Detection of an IM Drive Based on Both Time and Frequency Domain Analyses," in IEEE Transactions on Industry Applications, vol. 53, no. 4, pp. 4087-4096, July-Aug. 2017.
- [5] P. Vicente, J. Rodriguez, M. Negrea and A. Arkkio, "A general scheme for induction motor condition monitoring," 2005 5th IEEE International Symposium on Diagnostics for Electric Machines, Power Electronics and Drives, Vienna, 2005, pp. 1-6.
- [6] H. Razik, M. B. R. Correa and E. R. C. da Silva, "The use of particle swarm optimisation for the tracking of Induction motor faulty lines," 2009 International Conference on Power Engineering, Energy and Electrical Drives, Lisbon, 2009, pp. 680-684.
- [7] A. M. da Silva, R. J. Povinelli and N. A. O. Demerdash, "Induction Machine Broken Bar and Stator Short-Circuit Fault Diagnostics Based on Three-Phase Stator Current Envelopes," in IEEE Transactions on Industrial Electronics, vol. 55, no. 3, pp. 1310-1318, March 2008.
- [8] R. J. Romero-Troncoso et al., "FPGA-Based Online Detection of Multiple Combined Faults in Induction Motors Through Information Entropy and Fuzzy Inference," in IEEE Transactions on Industrial Electronics, vol. 58, no. 11, pp. 5263-5270, Nov. 2011.
- [9] M.R. Mehrjou, N. Mariun, N. Misron, M. A. M. Radzi, "Analysis of statistical features based on start-up current envelope for broken rotor bar fault detection in line start permanent magnet synchronous motor," Electrical Engineering, vol. 99, no 1, pp. 187-201, 2017.
- [10] A. Bellini, F. Filippetti, C. Tassoni and G. A. Capolino, "Advances in Diagnostic Techniques for Induction Machines," in IEEE Transactions on Industrial Electronics, vol. 55, no. 12, pp. 4109-4126, Dec. 2008.

- [11] L. A. Pereira, D. da Silva Gazzana and L. F. A. Pereira, "Motor current signature analysis and fuzzy logic applied to the diagnosis of short-circuit faults in induction motors," 31st Annual Conference of IEEE Industrial Electronics Society, 2005. IECON 2005, pp. 6 pp.-. 2005.
- [12] W. T. Thomson and M. Fenger, "Industrial application of current signature analysis to diagnose faults in 3-phase squirrel cage induction motors," Conference Record of 2000 Annual Pulp and Paper Industry Technical Conference (Cat. No.00CH37111), Atlanta, GA, USA, 2000, pp. 205-211.
- [13] M. E. H. Benbouzid and H. Nejari, "A simple fuzzy logic approach for induction motors stator condition monitoring," IEMDC 2001. IEEE International Electric Machines and Drives Conference (Cat. No.01EX485), Cambridge, MA, 2001, pp. 634-639.
- [14] S. Singh and N. Kumar, "Detection of Bearing Faults in Mechanical Systems Using Stator Current Monitoring," in IEEE Transactions on Industrial Informatics, vol. 13, no. 3, pp. 1341-1349, June 2017.
- [15] R. Puche-Panadero, M. Pineda-Sanchez, M. Riera-Guasp, J. Roger-Folch, E. Hurtado-Perez and J. Perez-Cruz, "Improved Resolution of the MCSA Method Via Hilbert Transform, Enabling the Diagnosis of Rotor Asymmetries at Very Low Slip," in IEEE Transactions on Energy Conversion, vol. 24, no. 1, pp. 52-59, March 2009.
- [16] H. El Bouchikhi, V. Choqueuse, M. Benbouzid and J. A. Antonino-Daviu, "Stator current demodulation for induction machine rotor faults diagnosis," 2014 First International Conference on Green Energy ICGE 2014, Sfax, 2014, pp. 176-181
- [17] A. Sapena-Baño, M. Pineda-Sanchez, R. Puche-Panadero, J. Martinez-Roman and Ž. Kanović, "Low-Cost Diagnosis of Rotor Asymmetries in Induction Machines Working at a Very Low Slip Using the Reduced Envelope of the Stator Current," in IEEE Transactions on Energy Conversion, vol. 30, no. 4, pp. 1409-1419, Dec. 2015.
- [18] M. E. H. Benbouzid and G. B. Kliman, "What stator current processing-based technique to use for induction motor rotor faults diagnosis?," in IEEE Transactions on Energy Conversion, vol. 18, no. 2, pp. 238-244, June 2003.
- [19] S.B. Salem, K. Bacha, A. Chaari, "Support vector machine based decision for mechanical fault condition monitoring in induction motor using an advanced Hilbert-Park transform," ISA transactions, vol. 51, no 5, pp. 566-572, 2012.
- [20] Zidani, M. E. H. Benbouzid, D. Diallo and M. S. Nait-Said, "Induction motor stator faults diagnosis by a current Concordia pattern-based fuzzy decision system," in IEEE Transactions on Energy Conversion, vol. 18, no. 4, pp. 469-475, Dec. 2003
- [21] Xu, L. Sun, L. Xu and G. Xu, "Improvement of the Hilbert Method via ESPRIT for Detecting Rotor Fault in Induction Motors at Low Slip," in IEEE Transactions on Energy Conversion, vol. 28, no. 1, pp. 225-233, March 2013.
- [22] Bessam a, A.Menacer b, M.Boumehraz a, H.Cherif , "Detection of broken rotor bar faults in induction motor at low load using neural network," ISA transactions, vol. 64, pp. 241-246. 2016.
- [23] Jaksch, "Faults diagnosis of three-phase induction motors using envelope analysis," 4th IEEE International Symposium on Diagnostics for Electric Machines, Power Electronics and Drives, 2003. SDEMPED 2003., 2003, pp. 289-293.
- [24] Elbouchikhi, V. Choqueuse, Y. Amirat, M. E. H. Benbouzid and S. Turri, "An Efficient Hilbert-Huang Transform-Based Bearing Faults Detection in Induction Machines," in IEEE Transactions on Energy Conversion, vol. 32, no. 2, pp. 401-413, June 2017.
- [25] A. Consoli, F. Gennaro, A. Raciti and A. Testa, "Fuzzy logic application to pre-fault diagnoses of induction motors," Proceedings of the 1998 Second IEEE International Caracas Conference on Devices, Circuits and Systems. ICCDCS 98. On the 70th Anniversary of the MOSFET and 50th of the BJT. (Cat. No.98TH8350), Isla de Margarita, 1998, pp. 249-254.
- [26] M. S. Ballal, Z. J. Khan, H. M. Suryawanshi and R. L. Sonolikar, "Adaptive Neural Fuzzy Inference System for the Detection of Inter-Turn Insulation and Bearing Wear Faults in Induction Motor," in IEEE Transactions on Industrial Electronics, vol. 54, no. 1, pp. 250-258, Feb. 2007.
- [27] B. Samanta, " Gear fault detection using artificial neural networks and support vector machines with genetic algorithms," Mechanical Systems and Signal Processing 18,pp.625-644, 2004.
- [28] P. Konar, P. Chattopadhyay, " Bearing fault detection of induction motor using wavelet and Support Vector Machines (SVMs) ," Applied Soft Computingvol. 11, no 6, pp. 4203-4211, 2011.
- [29] D.E Khodja, " Élaboration d'un système intelligent de surveillance et de diagnostic automatique en temps réel des défaillances des moteurs à induction," Thèse de doctorat,2007.
- [30] B. Saddam, A. Aissa, B. S. Ahmed and S. Abdellatif, "Detection of rotor faults based on Hilbert Transform and neural network for an induction machine," 2017 5th International Conference on Electrical Engineering - Boumerdes (ICEE-B), Boumerdes, 2017, pp. 1-6.